Optics Letters

Control of lateral thickness gradients of Mo–Si multilayer on curved substrates using genetic algorithm

Bo Yu,* Chunshui Jin, Shun Yao, Chun Li, Hui Wang, Feng Zhou, Benyin Guo, Yao Xie, Yu Liu, and Liping Wang

State Key Laboratory of Applied Optics, Changchun Institute of Optics and Fine Mechanics, Chinese Academy of Sciences, Changchun 130033, China
**Corresponding author: yubo@ciomp.ac.cn*

Received 8 June 2015; revised 20 July 2015; accepted 27 July 2015; posted 28 July 2015 (Doc. ID 242205); published 19 August 2015

An inversion method based on a genetic algorithm has been developed to control the lateral thickness gradients of a Mo–Si multilayer deposited on curved substrates by planar magnetron sputtering. At first, the sputtering distribution of the target is inversed from coating thickness profiles of flat substrates at different heights. Then, the speed profiles of substrates sweeping across the target are optimized according to the desired coating thickness profiles of the primary and secondary mirrors in a two-bounce projection system. The measured coating thickness profiles show that the non-compensable added figure error is below 0.1 nm rms, and the wavelength uniformity across each mirror surface is within ±0.2% P-V. The inversion method introduced here exhibits its convenience in obtaining the sputtering distribution of the target and efficiency in coating iterations during process development.

OCIS codes: (340.7480) X-rays, soft x-rays, extreme ultraviolet (EUV); (310.0310) Thin films; (230.4170) Multilayers; (340.0340) X-ray optics.

http://dx.doi.org/10.1364/OL.40.003958

Extreme ultraviolet lithography (EUVL) is a leading candidate for next-generation lithography. As extreme ultraviolet radiation is strongly absorbed by all materials and the refractive index of the materials is so close to unity, optical refractive elements cannot be used in EUVL optical systems, and therefore, an all-reflective optical system is essential. To improve the reflectivity, highly reflective, normal incidence multilayer coatings need to be deposited on optics. Commercial EUVL tools require multilayers with high-quality attributes, such as high reflectivity, low stress, high stability, and high uniformity [1]. For projection optics, extremely precise control of the lateral thickness gradients of multilayers is necessary for wavelength matching and figure preservation. Lateral thickness gradients can be realized by shadowing masks [2–4], the tilt of the substrate [5], and the control of the speed profile of the substrate moving across the vapor source [6–8]. In practice, speed profile control is preferable to masks, as it avoids needing to frequently replace the masks when the source distribution drifts [9].

In this Letter, a planar magnetron sputtering system with speed profile control is used to deposit laterally graded multilayers (radially symmetrical) on curved substrates. Before deposition, a model is employed to simulate the deposition process. The schematic diagram of the planar magnetron sputtering is shown in Fig. 1. The planetary rotation of the substrate can be described as follows (the target center is set as the origin coordinate):

$$x_s = R\cos\theta - R + r\cos\varphi$$
$$y_s = R\sin\theta + r\sin\varphi$$
$$z_s = h(r), \quad \theta = \omega t + \theta_0, \quad \varphi = \omega_s t + \varphi_0.$$

R is the revolution radius, r is the spin radius, θ is the revolution angle, φ is the spin angle, ω is the revolution speed, and ω_s is the spin speed. The coating thickness profile $T(r)$ is given by

$$T(r) = \iint \mathrm{d}A_T \int \frac{D(x_T, y_T) M \cos^k\alpha \cos\beta}{\rho^2}\mathrm{d}t$$
$$= \iint \mathrm{d}A_T \int \frac{D(x_T, y_T) M \cos^k\alpha \cos\beta}{\rho^2\omega(\theta)}\mathrm{d}\theta$$

$$\rho = |\overrightarrow{ST}|, \qquad \cos\alpha = \frac{h}{\rho}, \qquad \cos\beta = \frac{\overrightarrow{ST}\cdot\hat{n}}{\rho}$$

$$\hat{n} = (\cos\varphi\sin\gamma, \sin\varphi\sin\gamma, -\cos\gamma).$$

The substrate slope angle γ is defined as the angle between the normal angle of the substrate and the z direction. For a concave substrate, $-\pi/2 < \gamma < 0$; for a convex substrate, $0 < \gamma < \pi/2$. $D(x_T, y_T)$ is the sputtering yield distribution of the target, and M is the mask factor. If $\overrightarrow{ST}$ intersects with the mask or intersects with the substrate at another point, M is set to 0; otherwise, M is set to 1. $\omega(\theta)$ is the speed profile and in practice, it is a discrete function. The sweeping angle is divided into n equal segments (e.g., 0.1° for each segment),

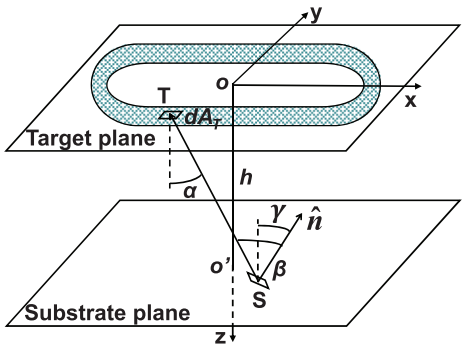

Fig. 1. Schematic diagram of planar magnetron sputtering.

and the sweeping speed in the jth segment is denoted as ω_j. Then, we have

$$T(r) = \sum_{j=1}^{n} \frac{1}{\omega_j} \int_{\theta_{j-1}}^{\theta_j} \mathrm{d}\theta \iint \frac{D(x_T, y_T) M \cos^k \alpha \cos \beta}{\rho^2} \mathrm{d}A_T.$$

Practically, a series of discrete points $\{r_i\}$ are chosen and the thickness series $\{T_i\}$ is calculated. Then, the thickness profile can be written as

$$T = \begin{pmatrix} T_1 \\ T_2 \\ \vdots \\ T_m \end{pmatrix} = \begin{pmatrix} S_{11}, S_{12}, \ldots, S_{1n} \\ S_{21}, S_{22}, \ldots, S_{2n} \\ \vdots \\ S_{m1}, S_{m2}, \ldots, S_{mn} \end{pmatrix} \begin{pmatrix} 1/\omega_1 \\ 1/\omega_2 \\ \vdots \\ 1/\omega_n \end{pmatrix} = S\Omega^{-1}$$

$$S_{ij} = \int_{\theta_{j-1}}^{\theta_j} \mathrm{d}\theta \iint \frac{D(x_T, y_T) M \cos^k \alpha \cos \beta}{\rho^2} \mathrm{d}A_T, \quad r = r_i. \tag{1}$$

Equation (1) gives the relationship between the thickness profile and the speed profile. The matrix S needs to be calculated once and then it is used in the process of finding the proper speed profile for the desired thickness profile. This matrix method accelerates the process of making the calculations.

To calculate the matrix S, the sputtering distribution of the source should be known first. The straightforward way is to measure the erosion profile of the target directly [10]. However, this method involves opening open the chamber and taking the targets down, which is time-consuming and inefficient. Here, we introduce a method to inverse the sputtering distribution of the source from the coating thickness distribution using a genetic algorithm (GA). The erosion area is supposed to be along a racetrack described by two parameters: L is the half-length of the straight portion, and R_T is the radius of the turnaround portion. The erosion profile perpendicular to the racetrack is described by the Gaussian function of distance to the center of racetrack $\exp(-0.5d^2/\sigma^2)$, and the angular distribution of the sputtered atoms is represented by $\cos^k \alpha$. So only four parameters, L, R_T, σ, and k, are used to characterize the sputtering distribution of the source. To reverse these parameters, the coating thickness profiles $T(r)$ of flat substrates ($\gamma = 0$) at several different heights can be utilized. The fitness function is defined as

$$F = \sum_{j=1}^{n} \sum_{i=1}^{m} |T_c(r_i, h_j)/T_c(r_1, h_1) - T_e(r_i, h_j)/T_e(r_1, h_1)|. \tag{2}$$

T_c is the calculated thickness profile from the sputtering parameters, and T_e is the experimental thickness profile. The sputtering parameters can be derived by minimizing the fitness function. Due to the local minima, it is not easy to reverse the sputtering parameters from the thickness profiles, and a global optimization method is necessary. Here, we choose a genetic algorithm as our reversing tool. A genetic algorithm is a stochastic method based on the model of natural evolution. The algorithm repeatedly modifies a population of individual solutions. At each step, it selects individuals randomly from the current population to be parents and uses them to produce children for the next generation with crossover and mutation rules [11]. To implement the inversion method mentioned above, we have developed a program that is written in FORTRAN and is adapted from a GA code written by Carroll [12]. The GA parameters that led to the most rapid convergence are chosen. Uniform crossover is performed using a tournament selection with a crossover probability of 0.5. The mutation rate is 0.02, the population is 100, and the number of generations is 50.

To test the sputtering distribution reversion method mentioned above, molybdenum and silicon (Mo–Si) single layers are deposited by a commercially available DC magnetron sputtering system from Leybold Optics (NESSY 1900). A detailed description of a similar system can be found elsewhere [13]. For each target, the thickness profiles $T(r)$ of the flat substrates at three different heights ($h = 65$, 75, and 85 mm) are used. The substrates sweep across the target at a constant revolution speed (~1 rpm) and spin speed (500 rpm) for several rounds to obtain a coating thickness close to 30 nm, which is a thickness suitable to be measured by grazing incidence x ray reflectivity. The x ray reflectivity is performed with a PANalytical X'Pert PRO MRD x ray diffractometer, with a working wavelength at 0.154 nm. The reversed sputtering parameters are summarized in Table 1. The third row shows the sputtering parameters of a virtual Mo–Si averaged target. The averaged thickness is calculated by $T_{\text{Mo-Si}}(r_i, h_j) = aT_{\text{Mo}}(r_i, h_j) + bT_{\text{Si}}(r_i, h_j)$. The thicknesses of the single layers are rescaled so that the corresponding Mo–Si multilayer has an effective Γ—ratio close to 0.4. The fitting results and the sputtering yield distribution of the Mo–Si averaged target are shown in Fig. 2.

After getting the sputtering distribution of the target, the next step is to find a proper speed profile for the designed coating thickness profile. A genetic algorithm is also used to solve this inversion problem. The fitness function is defined as

$$F = \sum_{i=1}^{m} |T_c(r_i, \omega(\theta)) - T_{\text{goal}}(r_i)|. \tag{3}$$

For simplicity, stepwise speed profiles are often used. The speed in each step and the transitional angle between two steps are the optimizing parameters. To compensate for the systematic deviation between the calculated and the experimental thickness profiles, iterations may be needed. The iteration is performed according to

$$T_{c,j+1} \to T_{\text{goal},j+1} = T_{c,j} + T_{\text{goal},0} - T_{e,j}. \tag{4}$$

Table 1. Reversed Sputtering Parameters

	L (mm)	R_T (mm)	σ (mm)	K
Mo	236.0	11.4	12.9	1.90
Si	224.8	25.3	8.9	2.36
Mo–Si	236.5	14.9	13.3	2.31

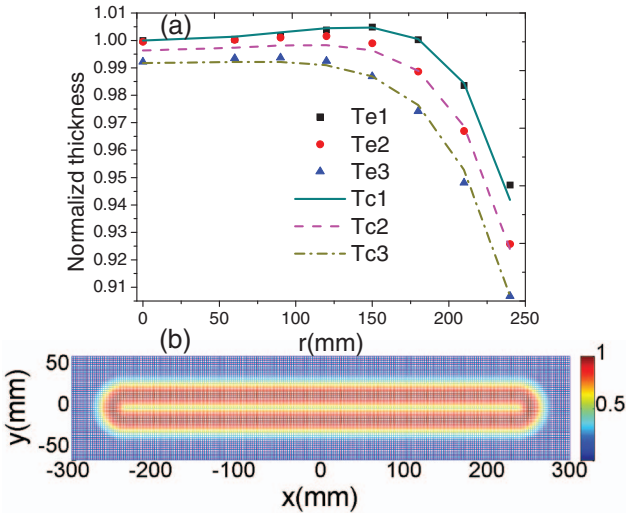

Fig. 2. (a) Fitted results of thickness profiles of flat substrates sweeping across the Mo–Si virtual target at heights of 65, 75, and 85 mm. (b) Reversed sputtering yields the distribution of the Mo–Si averaged target.

$T_{c,j}$ is the calculated thickness profile from the optimized speed profile, and $T_{e,j}$ is the experimental thickness profile in the jth iteration. $T_{\text{goal},0}$ is the designed thickness profile, and $T_{\text{goal},j+1}$ is the optimization target in the $(j+1)$th iteration.

To test the speed profile reversion algorithm, the convex primary (M1) and concave secondary (M2) mirrors in a two-bounce projection system are used. Both of them are rotationally symmetric aspheres with a maximum aspheric departure of a few micrometers. Their best-fit-spherical radii are 304.74 and 338.66 mm, respectively. The angles of incidence range from 2.4° to 8.5° across a clear aperture radius of 21–60 mm for M1 and from 0.3° to 1.9° across a clear aperture radius of 60–184 mm for M2. The lateral thickness gradients are designed for both the M1 and M2 mirrors to produce a phase and a centroid wavelength (of the reflectance versus wavelength curve) that remain constant at all locations within the mirror's clear aperture. According to the Bragg condition, multilayer wavelength and thickness are proportional. So the multilayer thickness profiles are determined by measuring the centroid wavelength at a fixed incidence angle across the mirror. All the extreme ultraviolet reflectance measurements in this Letter are performed by the CXUVS spectrometer from Bruker ASC. The spectrometer is capable of delivering extreme ultraviolet centriod wavelength results with 0.01% relative precision.

Following the optimization algorithms mentioned above, the coating processes for M1 and M2 are developed. The coating thickness profiles are optimized for two goals: low, noncompensable, added figure error (within 0.1 nm rms), and low, peak-to-valley variation from ideal profiles (with ±0.1% P-V). The non-compensable, added figure error of the multilayer coating is determined by the subtraction of a polynomial term $ar^2 + b$, which is entirely correctable via alignment shifts of the mirrors, from the total multilayer thickness profiles (normalized thickness profiles multiplied by 280 nm). As multilayer added figure errors introduce aberrations that can be detrimental to the overall performance of the imaging system, thickness profiles are optimized primarily for a low added figure error, rather than peak-to-valley (P-V) uniformity.

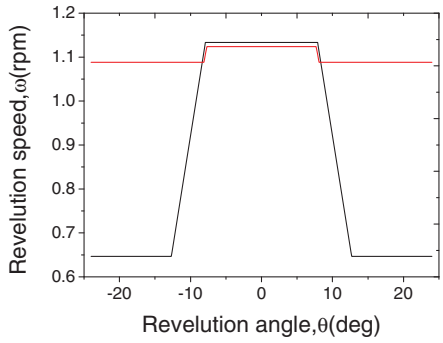

Fig. 3. Optimized speed profile for M1 (black curve) and M2 (red curve).

The optimized speed profiles of M1 and M2 are shown in Fig. 3. The angular sampling interval is 0.1° (segment width in calculating matrix S). For both mirrors, two-step speed profiles are used, and optimizations are performed with a constraint that the acceleration should be smaller than 0.2 rpm/deg. The corresponding measured coating thickness profiles are shown in Fig. 4. The non-compensable, added figure errors of the M1 and M2 multilayer coatings are determined to be 0.08 and 0.02 nm rms, respectively, within the 0.1 nm rms specification. To further confirm the low, non-compensable, added figure error of the M2 coating thickness profile, the surface figures of a spherical test substrate (best-fit spherical approximation of the actual M2 aspherical surface) before and after coating are

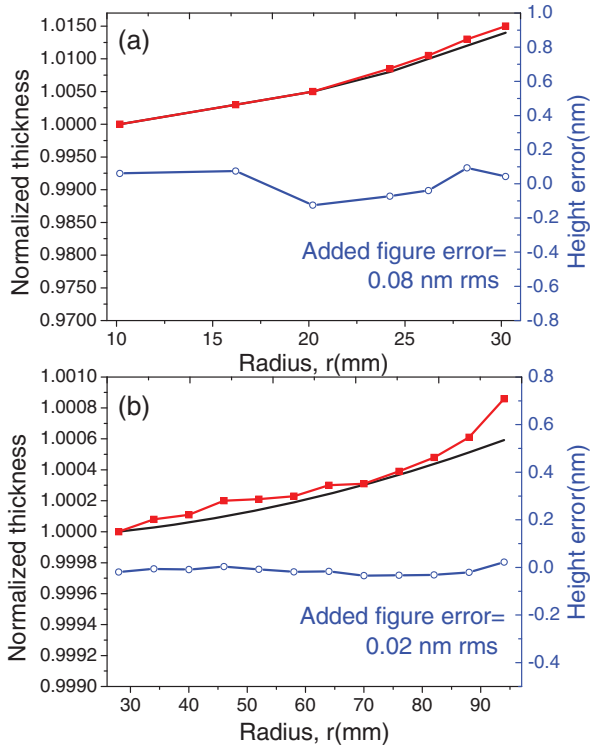

Fig. 4. Measured coating thickness profiles of (a) M1 and (b) M2. In each plot, the top two curves (left: y axis) are the measured thickness profile (square data points) and the designed thickness profile (solid curve). The bottom curve (right: y axis) represents the noncompensable, added figure error.

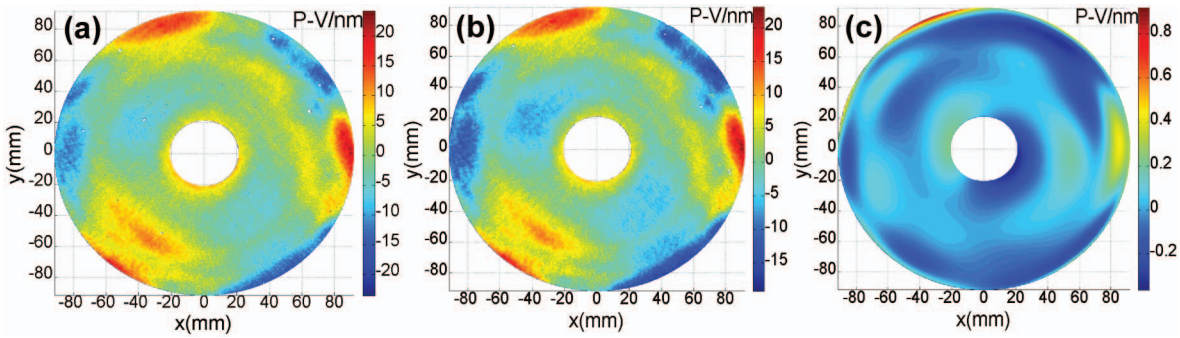

Fig. 5. The surface figures of a spherical test substrate for M2 (a) before coating, (b) after coating, and (c) the difference between the two figures.

measured by an interferometer. The results are shown in Fig. 5. The difference between the figures of the substrate before and after coating is fitted by Zernike polynomials (36 terms). After subtracting terms Z1–Z4 (piston, x tilt, y tilt, and focus), the remainder is smaller than 0.1 nm rms, in accordance with the extreme ultraviolet centriod wavelength result.

The extreme ultraviolet reflectance is measured at the fixed angle of incidence $\theta_m = 6°$. As M1 operates at $2.4° < \theta_i < 8.5°$, and M2 operates at $0.3° < \theta_i < 1.9°$, the wavelength at the actual angles of operation needs to be translated through the modified Bragg relation as follows:

$$\lambda_i = \lambda_m \sqrt{\cos^2 \theta_i - 2\delta} / \sqrt{\cos^2 \theta_m - 2\delta}. \quad (5)$$

$\delta = \Gamma\delta_{\mathrm{Mo}} + (1-\Gamma)\delta_{\mathrm{Si}} = 0.0762\Gamma + 0.0010(1-\Gamma)$, and the values of δ_{Mo} and δ_{Si} are taken from the website of the Center for X-Ray Optics. The translated wavelengths are plotted in Fig. 6. The wavelength uniformity across each mirror surface is within ±0.2% P-V. To reach the goal wavelength of 13.5 nm, the optimized speed profiles have been scaled by a certain factor.

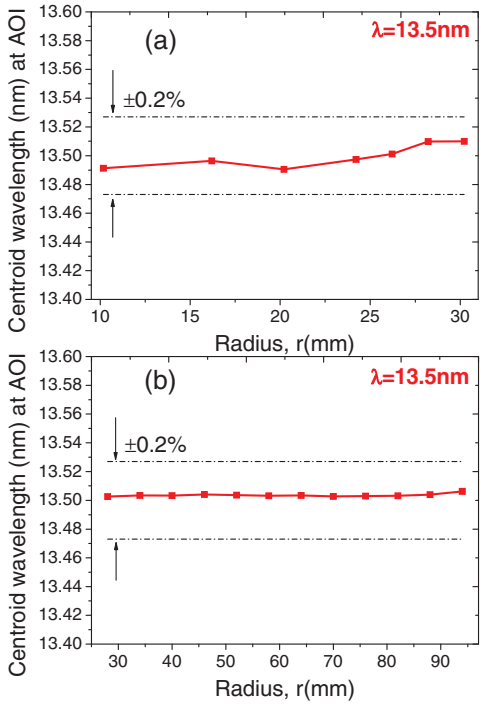

Fig. 6. The wavelength uniformity across the surface of (a) M1 and (b) M2.

It should be emphasized here that only several iterations are needed to reach the desired coating thickness profiles mentioned above. For mirror M1, the first speed profile can achieve the desired coating thickness profile, and no iteration is needed. For mirror M2, two iterations are needed. The small number of iterations indicates the efficiency of the genetic algorithm.

In summary, we have presented an inversion method based on a genetic algorithm to control the lateral thickness gradients of a Mo–Si multilayer deposited on curved substrates by planar magnetron sputtering. The sputtering distribution of the source can be derived by fitting the coating thickness profiles of flat substrates at different heights. There is no need to measure the source flux distribution or the erosion profile of the target, which is time-consuming and inconvenient. The genetic algorithm also shows its robustness and efficiency in finding the proper speed profile for the desired thickness profile.

Funding. National Science and Technology Major Project.

REFERENCES

1. E. Louis, A. E. Yakshin, T. Tsarfati, and F. Bijkerk, Prog. Surf. Sci. **86**, 255 (2011).
2. D. M. Broadway, Y. Y. Platonov, and L. A. Gomez, Proc. SPIE **3766**, 262 (1999).
3. J. B. Kortright, E. M. Gullikson, and P. E. Denham, Appl. Opt. **32**, 6961 (1993).
4. T. Foltyn, S. Braun, M. Moss, and A. Leson, Proc. SPIE **5193**, 124 (2004).
5. E. Spiller, S. L. Baker, P. B. Mirkarimi, V. Sperry, E. M. Gullikson, and D. G. Stearns, Appl. Opt. **42**, 4049 (2003).
6. R. Soufli, R. M. Hudyma, E. Spiller, E. M. Gullikson, M. A. Schmidt, J. C. Robinson, S. L. Baker, C. C. Walton, and J. S. Taylor, Appl. Opt. **46**, 3736 (2007).
7. C. Morawe and J. Peffen, Proc. SPIE **7448**, 1 (2009).
8. D. M. Broadway, M. D. Kriese, Y. Ya, and Y. Platonov, Proc. SPIE **4145**, 80 (2001).
9. C. Montcalm, C. C. Walton, and J. A. Folta, "Method and system using power modulation and velocity modulation producing sputtered thin films with sub-angstrom thickness uniformity or custom thickness gradients," U.S. patent 6,668,207 (December 23, 2003).
10. W. Schmid, "Construction of a sputtering reactor for the coating and processing of monolithic U-Mo nuclear fuel," dissertation (Technical University of Munich, 2011).
11. D. E. Goldberg, *Genetic Algorithms in Search, Optimization and Machine Learning* (Addison-Wesley, 1989).
12. D. L. Carroll, GA Driver: Free Vision, http://www.cuaerospace.com/Technology/GeneticAlgorithm/GADriverFreeVersion.aspx.
13. T. Feigl, S. Yulin, N. Benoit, and N. Kaiser, Microelectron. Eng. **83**, 703 (2006).